

Dynamics of Multi-Agent Actor-Critic Learning in Stochastic Games: from Multistability and Chaos to Stable Cooperation

Yuxin Geng¹, Wolfram Barfuss^{3,4,5}, Feng Fu^{6,7}, and Xingru Chen^{2*}

¹School of Mathematical Sciences, Beijing University of Posts and Telecommunications, Beijing 100876, China

²School of Artificial Intelligence, Beihang University, Beijing 100191, China

³Transdisciplinary Research Area Sustainable Futures, University of Bonn, Germany

⁴Center for Development Research, University of Bonn, Germany

⁵Institute for Food and Resource Economics, University of Bonn, Germany

⁶Department of Mathematics, Dartmouth College, Hanover, NH 03755, USA

⁷Department of Biomedical Data Science, Geisel School of Medicine at Dartmouth, Lebanon, NH 03756, USA

*Corresponding author: xingrucz@gmail.com

Abstract

Achieving robust coordination and cooperation is a central challenge in multi-agent reinforcement learning (MARL). Uncovering the mechanisms underlying such emergent behaviors calls for a dynamical understanding of learn processes. In this work, we investigate the dynamics of actor-critic agents in stochastic games, focusing on the impact of entropy regularization. By leveraging time-scale separation, we derive the system's evolution equations, which are then formally analyzed using dynamical systems theory. We find that in the constant-sum game of Matching Pennies, the system exhibits chaotic behavior. Entropy regularization mitigates this chaos and drives the dynamics toward convergence to fair cooperation. In contrast, in the general-sum game of the Prisoner's Dilemma, the system displays multistability. Interestingly, the three stable equilibria of the system correspond to the well-known ALLC (Always Cooperate), ALLD (Always Defect), and GRIM (Grim Trigger) strategies from evolutionary game theory (EGT). Entropy regularization strengthens system resilience by enlarging the basin of attraction of the cooperative equilibrium. Our findings reveal a close link between the mechanism of direct reciprocity in EGT and how cooperation emerges in MARL, offering insights for designing more robust and collaborative multi-agent systems.

Keywords: cooperation, multi-agent reinforcement learning, stochastic games, evolutionary game theory.

1 Introduction

Intelligence in both biological and artificial systems is characterized by the ability to learn and adapt [36]. Reinforcement learning (RL) provides a general framework for discovering optimal strategies in dynamic and uncertain environments [44]. Its effectiveness has been demonstrated across diverse fields, including neuroscience, sociology, physics, and computer science, particularly artificial intelligence [10, 25, 39, 42, 34]. A core challenge in RL is to learn efficiently without access to a complete model of the environment. To address this, various model-free algorithms have been developed that enable agents to refine both their value estimates of environmental

states and actions and behavioral policies directly from experience. Among these, temporal difference (TD) learning stands out as a foundational method that combines ideas from dynamic programming and Monte Carlo methods [43]. By updating value estimates based on prediction errors, TD learning allows agents to learn from partial episodes and underpins many modern RL algorithms, including SARSA, Q-learning, and actor-critic (AC) methods [51, 24].

Extending the RL paradigm to populations of interacting decision-makers gives rise to *multi-agent reinforcement learning* (MARL), which studies how autonomous agents learn and adapt in shared environments where the outcomes of actions depend on others' choices. It bridges RL with ideas from game theory, control, and complex systems, providing a framework for modeling both competition and cooperation among agents [8, 46, 33]. In MARL, each agent interacts not only with a dynamic environment but also with peers whose policies co-evolve over time. This coupling introduces inherent *non-stationarity*, in the sense that the distributions governing state transitions and rewards shift as other agents refine their behaviors [52]. As a result, classical convergence guarantees from single-agent RL no longer hold, leading to instability, oscillation, or even collapse during training [54]. At the same time, MARL systems also exhibit rich emergent collective behaviors: agents optimizing for individual rewards can spontaneously develop sophisticated cooperative conventions and social norms, despite these behaviors not being explicitly encoded in the game's rules or reward structures [26, 22, 11, 31].

Unraveling the mechanisms behind such emergent phenomena in MARL requires investigating the underlying learning dynamics [5]. In this work, we focus on the AC learning paradigm, which has achieved remarkable success in both single-agent and cooperative settings, yet remains less well understood in mixed-motive and competitive environments [30, 12, 53]. Unlike value-based methods such as Q-learning, AC algorithms maintain both a value estimator (the critic) and a parameterized policy (the actor). The critic guides the actor's policy improvement, which in turn reshapes the value landscape. Building on the classical Advantage Actor-Critic (A2C) algorithm [30], subsequent studies have refined AC algorithms primarily from an optimization perspective. For instance, Trust Region Policy Optimization (TRPO) constrains policy updates within a trust region to guarantee monotonic improvement [37], while Proximal Policy Optimization (PPO) replaces the hard constraint of TRPO with a clipped surrogate objective [38].

Beyond these algorithmic advances, we analyze the learning dynamics of AC algorithms in multi-agent settings from the perspective of dynamical systems. Since AC methods optimize policies along the gradient of performance, prior research has revealed that they often converge to deterministic and suboptimal strategies [28, 41, 30, 14]. To encourage sustained exploration, an entropy-regularization term is added to the objective function [14, 9]. However, the effect of this additional component on the collective dynamics of interacting agents remains poorly understood, especially regarding its role in promoting and stabilizing cooperative behavior [1]. To address this gap, we formalize entropy-regularized A2C learning within the framework of stochastic games [40] and derive a set of ordinary differential equations (ODEs) that govern the evolution of each agent's policy. Our formulation allows for a detailed analysis of the learning trajectories through theoretical tools of dynamical systems, including a detailed characterization of the equilibria, stability, and bifurcation structure. The framework is then applied to two representative examples: the constant-sum game of two-state Matching Pennies (MP) and the general-sum game of two-state Prisoner's Dilemma (PD) [16, 17].

In the two-state MP, the unregularized system contains no stable equilibrium. As the discount factor γ increases, the learning trajectories transition from strictly periodic orbits to quasi-periodic motion and eventually to chaos. This chaotic regime introduces inherent unpredictability, destabilizing cooperative outcomes. Entropy regularization suppresses this instability and steers the system toward convergence to fair and balanced cooperation. In contrast, in the two-state PD, the system admits three stable equilibria that correspond to classical strategies from Evolutionary Game Theory (EGT): ALLC (Always Cooperate), ALLD (Always Defect), and GRIM (Grim Trigger) [2, 13]. Surprisingly, the stability condition of the GRIM equilibrium

coincides with the principle of direct reciprocity, a key mechanism in EGT that explains the emergence of cooperation among self-interested individuals [32]. Moderate exploration through entropy regularization further enhances resilience by preventing convergence to mutual defection and expanding the basin of attraction of the cooperative equilibrium.

The condition for direct reciprocity to favor cooperation is that the probability of future encounters exceeds the cost-to-benefit ratio of the cooperative action. In reinforcement learning, the discount factor plays an analogous role by quantifying how strongly agents value future rewards [26, 4]. Hence, cooperation emerges only when agents sufficiently prioritize long-term outcomes. The correspondence between these two domains shows that the emergence of cooperative behavior in MARL is not an isolated phenomenon but arises from the same fundamental principles that foster cooperation in biological and social systems. Extending this analogy, entropy regularization in MARL can be interpreted as a mutation mechanism in EGT, which has been shown to promote cooperation under direct reciprocity [45, 21]. Together, these insights establish a unified theoretical bridge between MARL and EGT and lay a conceptual foundation for designing cooperative and resilient multi-agent systems.

2 Related Works

In the pioneering work of Börgers and Sarin [7], the continuous-time limit of cross-learning dynamics was shown to be equivalent to the replicator dynamics (RD). This connection between RL and EGT uncovers a common mathematical foundation underlying two seemingly distinct paradigms [49]. In the language of EGT, individuals with higher fitness are more likely to reproduce and propagate their phenotype in subsequent generations, whereas in RL terminology, actions yielding higher rewards are selected with higher probability at the next training step. Tuyls et al. extended this framework to myopic Q-learning in normal-form games [47], and Kianercy and Galstyan thoroughly examined its dynamics for two-player, two-action normal-form games [23]. Subsequent work generalized these learning models to population games, where mean-field approximation is employed to derive the dynamics at the population level [19, 50, 20].

The aforementioned studies mainly focus on normal-form games, assuming that the environmental state remains static during the learning process. Nevertheless, real-world scenarios often involve dynamic environments in which agents’ actions influence not only their immediate rewards but also the state of the environment. This creates a more intricate learning problem, requiring agents to develop state-dependent policies that balance short-term rewards against long-term objectives [27]. To address such dynamics, several extensions have been proposed, including Piecewise RD [48], state-coupled RD [17], and RESQ-learning [16]. More recently, Barfuss et al. introduced a methodological framework that separates the interaction and update processes in MARL. They derived the deterministic limit of TD learning in stochastic games and revealed diverse discrete-time dynamical regimes [3]. Inspired by this line of work, we further apply the two-timescale analysis to AC learning, where agents interact extensively with the environment and perform batch updates. The critic adapts rapidly (on a fast timescale) to provide accurate value estimations, while the actor evolves gradually (on a slow timescale) to refine its policy based on the critic’s evaluations.

3 Model

We study MARL in dynamic environments modeled as stochastic games, which formally capture both the interactions among agents and the evolution of environmental states. Each agent independently learns via the A2C algorithm augmented with entropy regularization. The main components of our framework are defined in the following subsections, and the corresponding pseudocode is presented in Algorithm 1.

3.1 Stochastic Games

A natural and flexible framework for modeling dynamic environments is the stochastic game, defined by the tuple $(\mathcal{N}, \mathcal{S}, \mathcal{A}, T, R)$. Here, a collection of agents $\mathcal{N} = \{1, 2, \dots, N\}$ interacts within an environment characterized by a finite set of states $\mathcal{S} = \{s_1, s_2, \dots, s_K\}$. At each time step, each agent selects from a set of actions $\mathcal{A} = \{a_1, a_2, \dots, a_M\}$. Specifically, each agent i samples an action $a(i)$ according to its own policy $X(i, s, a)$, which assigns a probability to each action a in state s . For notational clarity, we let subscripts denote environmental quantities, e.g., a_m or s_k , whereas parentheses denote quantities for agent i , e.g., $a(i)$ represents agent i 's action. The joint action $\mathbf{a} = [a(1), a(2), \dots, a(N)]$, together with the current state $s \in \mathcal{S}$, determines the transition probability $T(s, \mathbf{a}, s')$ to the next state $s' \in \mathcal{S}$. The reward obtained by agent i from this interaction is given by the utility function $R(i, s, \mathbf{a}, s')$.

3.2 Entropy-Regularized Actor-Critic Learning

We assume that each agent i aims to maximize the following objective function:

$$J(i) = \mathbb{E}_\tau \left\{ \sum_{t=0}^{\infty} \gamma^t [r_t(i) - \eta \log X(i, s_t, a_t(i))] \right\}. \quad (1)$$

The first term represents the discounted cumulative reward, averaged over all possible trajectories τ . The second term corresponds to the negative log-likelihood form of entropy regularization, based on the entropy definition

$$\mathcal{H}[X(i, s, \cdot)] = \sum_a -X(i, s, a) \log X(i, s, a). \quad (2)$$

When the entropy coefficient $\eta = 0$, the objective reduces to pure exploitation, meaning that the agent maximizes only the discounted return without any incentive to explore. In contrast, a positive entropy coefficient $\eta > 0$ encourages exploration by promoting more stochastic policies. As we will demonstrate, entropy regularization can steer the system away from chaotic dynamics and inefficient mutual defection, guiding it toward stable cooperative behavior.

Agents employ the entropy-regularized A2C algorithm to optimize their objective function, using samples obtained from continual interactions with the environment [30, 3]. The learning framework consists of two components: the actor and the critic. The actor is the decision maker, parameterized by $\boldsymbol{\theta}$, which defines the policy $X(i, s, a)$. In function approximation scenarios, such as when the actor is implemented as a neural network, the system dynamics depend on the specific choice of approximator, including its architecture. For analytical tractability, we adopt a tabular representation, where action selection follows Boltzmann exploration with temperature β :

$$X(i, s, a) = \frac{\exp[\beta \boldsymbol{\theta}^T \boldsymbol{\phi}(i, s, a)]}{\sum_{a' \in \mathcal{A}} \exp[\beta \boldsymbol{\theta}^T \boldsymbol{\phi}(i, s, a')]} \quad (3)$$

The parameter tensor $\boldsymbol{\theta}$ has dimension $N \times K \times M$, where $\theta(i, s, a)$ is associated with agent i and state-action pair (s, a) . The one-hot feature vector $\boldsymbol{\phi}(i, s, a)$ shares the same dimension as $\boldsymbol{\theta}$, taking the value 1 at the component corresponding to (i, s, a) and 0 elsewhere.

Meanwhile, the critic is the evaluator, estimating the value $V(i, s)$ for each state s to improve the performance of both the actor and the critic itself. After B interactions with the environment, each sample $(s, a(i), r(i), s')$ is used to compute the advantage function:

$$A(i) = r(i) + \gamma V(i, s') - V(i, s). \quad (4)$$

Intuitively, $V(i, s)$ serves as a baseline estimate of the return for state s . A positive advantage $A(i)$ indicates that the chosen action $a(i)$ outperforms this baseline, whereas a negative advantage implies underperformance.

Algorithm 1 Multi-Agent Entropy-Regularized Actor–Critic in Stochastic Games

```

1: Input: Stochastic game  $\mathcal{G} = (\mathcal{N}, \mathcal{S}, \mathcal{A}, T, R)$ ; maximum time steps  $T$ ; batch size  $B$ ; discount
   factor  $\gamma$ ; learning rates  $\alpha, \kappa$ ; entropy coefficient  $\eta$ ; inverse temperature  $\beta$ 
2: Initialize the actor  $\theta(i, s, a)$  and critic  $V(i, s)$  for each agent  $i$ , state  $s$ , and action  $a$ 
3: for  $t = 0$  to  $T - 1$  do
4:   Reset replay buffers:  $\mathcal{R}(i, s, a) \leftarrow \emptyset$  for all  $i, s$ , and  $a$ 
5:   for  $b = 1$  to  $B$  do
6:     Observe state  $s$ 
7:     for each agent  $i \in \mathcal{N}$  do
8:       Sample  $a(i)$  according to Equation (3)
9:     end for
10:    Execute joint action  $\mathbf{a}$ ; observe next state  $s'$  and reward  $r(i)$  for each agent  $i \in \mathcal{N}$ 
11:    for each agent  $i \in \mathcal{N}$  do
12:       $A(i) \leftarrow r(i) + \gamma V(i, s') - V(i, s)$ 
13:       $\mathcal{R}(i, s, a(i)) \leftarrow \mathcal{R}(i, s, a(i)) \cup \{(s, a(i), r(i), s', A(i))\}$ 
14:    end for
15:     $s \leftarrow s'$ 
16:  end for
17:  for each agent  $i \in \mathcal{N}$  do
18:    update  $V(i, s)$  according to Equation (5) for all  $s$ 
19:    update  $\theta(i, s, a)$  according to Equation (6) for all  $s$  and  $a$ 
20:     $\mathcal{R}(i, s, a) \leftarrow \emptyset$  for all  $s$  and  $a$ 
21:  end for
22: end for

```

The advantage estimates, together with the entropy regularization terms, are used to update the actor’s parameters in the direction of the policy gradient. Simultaneously, the critic updates its value estimates via a standard temporal-difference rule:

$$V(i, s) \leftarrow V(i, s) + \kappa \frac{1}{\sum_a |\mathcal{R}(i, s, a)|} \sum_{\mathcal{R}(i, s, a)} A(i, s, a), \quad (5)$$

$$\theta(i, s, a) \leftarrow \theta(i, s, a) + \alpha \frac{1}{|\mathcal{R}(i, s, a)|} \sum_{\mathcal{R}(i, s, a)} \{ \ast \}, \quad (6)$$

$$\{ \ast \} = \frac{\partial [\log X(i, s, a)]}{\partial \theta(i, s, a)} [A(i, s, a) - \eta \log X(i, s, a)].$$

Here, α and κ denote the learning rates for the actor and critic, respectively, and $\mathcal{R}(i, s, a)$ represents the set of all samples corresponding to state s and action a for agent i .

4 A2C Learning in Stochastic Games

Under typical training conditions, small batch sizes amplify stochastic effects, as agents must contend with the inherent randomness in both state transitions and policy sampling. Moreover, since agents update their policies after limited interactions, they may form inaccurate value estimates, leading to suboptimal policy updates and systematic biases in the learning dynamics. To overcome these analytical challenges and gain deeper theoretical insights into multi-agent learning, we adopt a **time-scale separation** approach, which decouples the interaction process, the critic’s update, and the actor’s update [3, 35]. By intuition, it allows agents to more thoroughly perceive the environment, acquiring sufficient information about state transitions,

reward structures, and the behavioral patterns of other agents to generate consistent and stable learning gradients. Formally, the separation of time scales is realized through two conditions: (1) a large batch size B , which allows agents to accumulate extensive interaction experiences before updating their value functions, and (2) small learning rates α and κ , with $\alpha \ll \kappa$, ensuring that policy updates occur gradually relative to rapid value updates.

As a result, agents can accurately estimate both the advantage function and the learning gradients. In this deterministic regime, the learning dynamics become amenable to analysis utilizing dynamical systems theory. The derivation of closed-form expressions is allowed for equilibrium points, stability conditions, and phase portraits that would otherwise be intractable in the original stochastic regime. On the fast time scale, the value functions quickly converge to their stationary forms, given by the Bellman equations:

$$\begin{aligned}\bar{V}_t(i, s) &= \mathbb{E}_{\mathbf{a}, s'} [R(i, s, \mathbf{a}, s') + \gamma \bar{V}_t(i, s')] \\ &= \sum_{\mathbf{a}, s'} \left[\prod_j X(j, s, a) \right] T(s, \mathbf{a}, s') [R(i, s, \mathbf{a}, s') + \gamma \bar{V}_t(i, s')],\end{aligned}\quad (7)$$

and

$$\begin{aligned}\bar{Q}_t(i, s, a) &= \mathbb{E}_{\mathbf{a}^{-i}, s'} [R(i, s, a + \mathbf{a}^{-i}, s') + \gamma \bar{V}_t(i, s')] \\ &= \sum_{\mathbf{a}^{-i}, s'} \left[\prod_{j \neq i} X(j, s, a) \right] [R(i, s, a + \mathbf{a}^{-i}, s') + \gamma \bar{V}_t(i, s')].\end{aligned}\quad (8)$$

Here, \mathbf{a}^{-i} denotes the joint action of all agents except agent i , and $+$ indicates concatenation. The actor's policy updates can further be expressed entirely in terms of the above quantities. In particular, the advantage function $\bar{A}_t(i, s, a)$ can be written as

$$\bar{A}_t(i, s, a) = \bar{Q}_t(i, s, a) - \bar{V}_t(i, s). \quad (9)$$

4.1 Evolutionary Interpretation of Policy Dynamics

To examine the temporal evolution of agent behavior, we shift the analysis from the parameter space to the policy space. Substituting Equations (6) and (9) into Equation (3), we obtain the discrete-time dynamics of the policy

$$X_{t+1}(i, s, a) \propto X_t(i, s, a) \exp \{ \alpha \beta [\bar{A}_t(i, s, a) - \eta \log X_t(i, s, a)] \}. \quad (10)$$

Here, the notation \propto indicates that the left-hand side is proportional to the right-hand side, with normalization applied over all possible actions. For a small learning rate α , we can expand the right-hand side around $\alpha = 0$. After straightforward algebraic manipulation, we derive the continuous-time dynamics of the policy:

$$\begin{aligned}\frac{d}{dt} X(i, s, a) &= \underbrace{\alpha \beta X(i, s, a) [\bar{Q}(i, s, a) - \bar{V}(i, s)]}_{\text{exploitation / selection}} \\ &\quad + \underbrace{\alpha \beta \eta X(i, s, a) \left\{ -\log X(i, s, a) - \mathcal{H}[X(i, s, \cdot)] \right\}}_{\text{exploration / mutation}}.\end{aligned}\quad (11)$$

Here, for notational simplicity, we omit the time subscript t . Notably, Equation (11) is mathematically equivalent to RD in EGT, which decomposes the actor's learning dynamics into two interpretable components. In the EGT framework, the policy of agent i in state s can be viewed as a population, where each action a represents a phenotype. The **selection** term increases the frequency of phenotypes with higher advantage values, analogous to exploitation in RL. The entropy-regularization term, on the other hand, plays the role of **mutation**, preserving population diversity. In the RL interpretation, it promotes exploration by encouraging agents to sample alternative actions and thereby discover potentially superior strategies.

Moreover, all boundaries of the policy space where $X(i, s, a) \in \{0, 1\}$ are equilibria of the system. When $\eta = 0$, the interior equilibria satisfy

$$\bar{Q}(i, s, a) = \bar{V}(i, s), \quad \text{for all } i, s, \text{ and } a. \quad (12)$$

In contrast, for $\eta > 0$, setting $dX(i, s, a)/dt = 0$ yields interior equilibria that coincide with the quantal response equilibria (QRE) [29], defined as

$$X(i, s, a) = \frac{\exp\{\bar{Q}(i, s, a)/\eta\}}{\sum_{a' \in \mathcal{A}} \exp\{\bar{Q}(i, s, a')/\eta\}}. \quad (13)$$

For notational simplicity, we use \mathbf{X} to denote the joint policy of all agents at equilibrium:

$$\mathbf{X} = [X(1, s_1, a_1), X(1, s_1, a_2), \dots, X(N, s_K, a_M)]. \quad (14)$$

The following theorem characterizes the stability of an equilibrium point \mathbf{X} located on the boundary of the policy space. It offers intuitive insights into how cooperation may emerge in the two-state PD game, which will be discussed later. The proof is provided in the Appendix.

Theorem 1. *When $\eta = 0$, the stability of the boundary equilibrium points of Equation (11) depends solely on the Q-value gaps. Specifically, for an equilibrium point \mathbf{X} satisfying $X(i, s, a) \in \{0, 1\}$ for all i, s , and a , the point is asymptotically stable if and only if the following condition holds for all i, s , and a :*

$$X(i, s, a) = 1 \iff \bar{Q}(i, s, a) > \bar{Q}(i, s, a'), \quad \text{for all } a' \neq a. \quad (15)$$

4.2 Effect of Entropy Regularization

To further investigate how entropy regularization affects the stability of the system, we perform a coordinate transformation by defining $Y(i, s, a) = \log X(i, s, a)$, which maps Equation (11) from the probability simplex to the logarithmic coordinate space:

$$\begin{aligned} \frac{d}{dt} Y(i, s, a) &= \alpha\beta [\bar{Q}(i, s, a) - \bar{V}(i, s)] + E(i, s, a), \\ E(i, s, a) &= \alpha\beta\eta \left[-Y(i, s, a) + \sum_{a'} X(i, s, a')Y(i, s, a') \right]. \end{aligned} \quad (16)$$

This coordinate change reshapes the geometry of the policy space, rendering the dynamics linear in both \bar{Q} and Y . More importantly, it enables an elegant closed-form characterization of the contraction property through the divergence as follows, whose proof is provided in the Appendix.

Theorem 2. *The divergence of the entropy term in Equation (16) is*

$$\sum_{i, s, a} \frac{\partial}{\partial Y(i, s, a)} \left[\frac{d}{dt} E(i, s, a) \right] = -NK(M-1)\alpha\beta\eta. \quad (17)$$

Consequently, entropy regularization imposes a strictly negative divergence effect on the original system.

According to Liouville's theorem, the divergence of a vector field quantifies the rate of change of volume in the phase space, that is, how an infinitesimal region of initial conditions expands or contracts over time. The regularization term contributes a strictly negative divergence of $-NK(M-1)\alpha\beta\eta$, indicating a dissipative effect that continuously contracts the volume in the logarithmic coordinate space. In vanilla A2C with $\eta = 0$, this dissipative mechanism is absent. Hence, there is no intrinsic process to dampen oscillations or suppress perturbations. As we will show later, in the MP game without entropy regularization, A2C players can exhibit chaotic

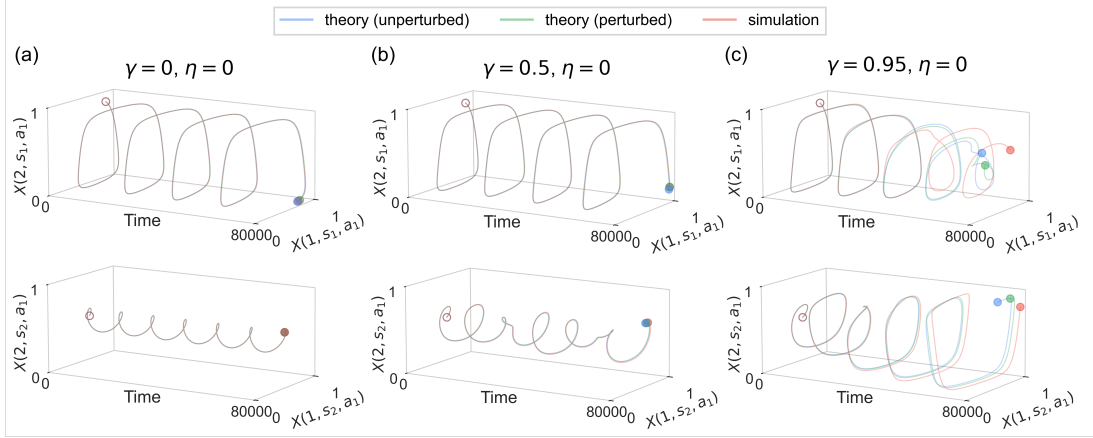


Figure 1: Policy evolution in the two-state Matching Pennies game without entropy regularization. For each parameter combination, the subfigure displays the trajectories of the two players’ policies in state s_1 and s_2 , respectively.

behavior: even infinitesimal perturbations can lead to vastly different trajectories, making the long-term behavior of the system fundamentally unpredictable.

As the regularization parameter η increases, the system exhibits stronger dissipation. Once the contracting effect induced by the entropy regularization term outweighs any expansive effect from the selection term, the volume in the phase space is guaranteed to shrink over time. Consequently, the long-term dynamics collapse onto attractors of lower dimensionality, typically stable fixed points. In the context of MARL, entropy regularization is often introduced as a heuristic to encourage exploration, yet it also serves as a powerful stabilizing force that drives agents’ policies toward steady configurations rather than allowing them to cycle indefinitely through unpredictable updates. In two-player, two-action normal-form games, the dynamics reduces to a two-dimensional system. By the Poincaré–Bendixson theorem, the presence of entropy regularization eliminates the possibility of limit cycles, ensuring that all trajectories converge to a stable fixed point [23]. In the two-state MP game examined in this work, entropy regularization likewise suppresses chaotic oscillations and stabilizes the interior equilibrium.

5 Results & Experiments

We now turn to empirical validation of the learning dynamics discussed above. Specifically, we examined how agents adapt their policies under entropy-regularized A2C in two illustrative two-state games.

5.1 Two-State Matching Pennies

As a representative constant-sum game, we consider the two-state MP game, involving two agents 1 and 2 and two states s_1 and s_2 . In both states, each agent can choose between two actions a_1 and a_2 . The environment transitions between states whenever agent 1 selects action a_1 . We represent the reward structure using the payoff matrices $\mathbf{U}(s)$, where, with agent 1 as the row player and agent 2 as the column player, each entry specifies the pair of payoffs received by the agents for a given joint action:

$$\mathbf{U}(s_1) = \begin{pmatrix} a_1 & a_2 \\ a_1 & (1, 0) & (0, 1) \\ a_2 & (0, 1) & (1, 0) \end{pmatrix}, \quad \mathbf{U}(s_2) = \begin{pmatrix} a_1 & a_2 \\ a_1 & (0, 1) & (1, 0) \\ a_2 & (1, 0) & (0, 1) \end{pmatrix}. \quad (18)$$

In state s_1 , matching actions yield a payoff of 1 for agent 1 and 0 for agent 2, while mismatched actions reverse these payoffs. In state s_2 , the reward structure is inverted.

We present the simulation trajectories in red alongside the theoretical predictions in blue derived from Equation (11) in Figure 1. In subfigure (a), for myopic learning agents with $\gamma = 0$, the trajectories of both agents' policies are strictly periodic. In this special case, the learning dynamics for each state are decoupled, exhibiting a conservative, Hamiltonian-like structure within each state's policy subspace.

In subfigure (b), with a positive discount factor $\gamma = 0.5$, the policy evolution in the two states becomes coupled through the advantage function. This dependency breaks the Hamiltonian structure observed for $\gamma = 0$. As a result, the trajectories no longer form simple closed loops but instead trace more intricate paths on the surface of a torus in the joint policy space. Despite the increased complexity, the agent-based simulation remains in close agreement with the theoretical predictions. In subfigure (c), for $\gamma = 0.95$, the simulation trajectories initially follow the theoretical predictions but gradually diverge and become increasingly unpredictable over time. This divergence does not reflect a failure of our model. Instead, it arises from chaotic behavior. The stochasticity and numerical noise in the agent-based simulations act as small perturbations that are exponentially amplified, producing deviations from the theoretical predictions.

To provide stronger empirical evidence of this chaotic behavior, we investigate the system's sensitivity to initial conditions by introducing a minuscule perturbation of magnitude 10^{-3} to the initial state and plotting the theoretical trajectory in green. For $\gamma = 0$ and $\gamma = 0.5$, the perturbed trajectory remains indistinguishable from the original one. In contrast, for $\gamma = 0.95$, the perturbed trajectory gradually deviates from the original orbit.

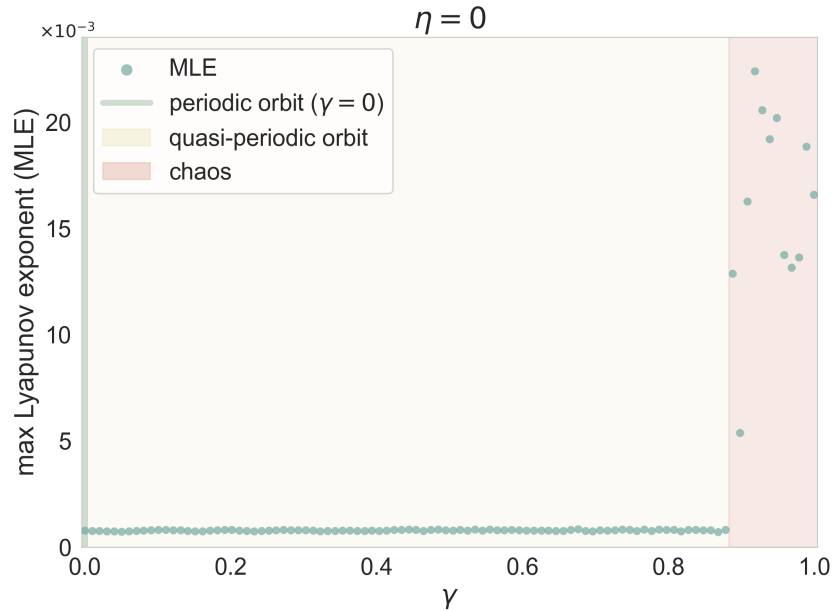


Figure 2: Maximum Lyapunov exponent (MLE) of the two-state Matching Pennies game without entropy regularization. The scattered points represent the MLE values for different values of γ , quantifying the sensitivity of agents' trajectories to small perturbations in initial conditions.

The above empirical evidence is further validated by computing the maximum Lyapunov exponent (MLE) λ for different values of γ , as shown in Figure 2. The MLE quantifies the average exponential rate at which infinitesimally close trajectories diverge over time. Formally, it is defined as the limit of the logarithmic growth rate of the separation between two initially

nearby trajectories $\mathbf{X}(t = 0)$ and $\mathbf{X}'(t = 0) = \mathbf{X}(t = 0) + \boldsymbol{\delta}$:

$$\lambda(\mathbf{X}(t = 0)) = \lim_{T \rightarrow \infty} \lim_{\|\boldsymbol{\delta}\| \rightarrow 0} \frac{1}{T} \log \frac{\mathbf{X}'(t = T) - \mathbf{X}(t = T)}{\mathbf{X}'(t = 0) - \mathbf{X}(t = 0)}. \quad (19)$$

A sharp bifurcation occurs at a critical threshold of γ . Below this threshold, the MLE is zero, indicating stable and predictable motion. Above the threshold, the MLE becomes positive, implying that initially close trajectories diverge exponentially over time. This behavior aligns with the divergence observed in Figure 1 (c).

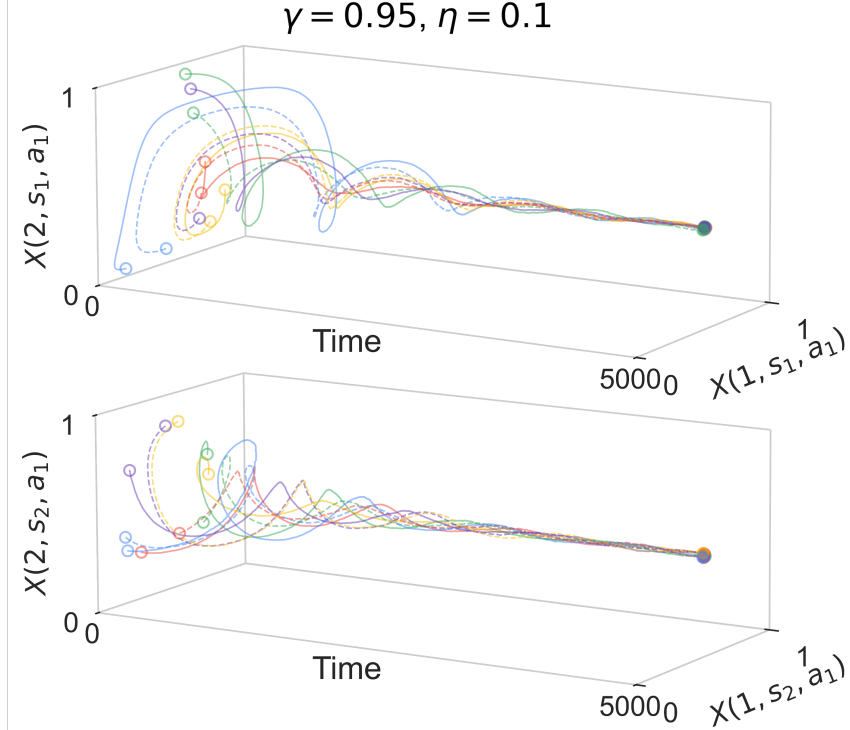


Figure 3: Policy evolution in the two-state Matching Pennies game with entropy regularization. Each subfigure shows ten simulation trajectories of the two players’ policies in state s_1 and s_2 , respectively, with trajectories initialized from random starting points.

Although multiple equilibria exist in the policy space when entropy regularization is absent, computing the eigenvalues of the Jacobian matrix of Equation (11) reveals that *none* of them are stable when $\gamma = 0$. In other words, unless the system is initialized precisely at an equilibrium, agents’ policies undergo perpetual oscillations. By comparison, when $\eta > 0$, the inner equilibrium $X(i, s, a) \equiv 1/2$ becomes globally attractive, as illustrated in Figure 3. The dissipative effect introduced by entropy regularization drives the system toward convergence, fostering fair cooperation characterized by equal payoffs.

5.2 Two-State Prisoner’s Dilemma

To investigate the emergence of cooperation under AC learning, we consider the general-sum two-state PD game [18, 48, 17, 16, 3]. The game involves two agents, labeled as 1 and 2, and two states s_1 and s_2 . Each state is a standard PD game, where agents can choose between cooperation (a_1) and defection (a_2). The payoff matrices are given by

$$\mathbf{U}(s_1) = \begin{pmatrix} a_1 & a_2 \\ b_1 - c & -c \end{pmatrix}, \quad \mathbf{U}(s_2) = \begin{pmatrix} a_1 & a_2 \\ b_2 - c & -c \end{pmatrix}, \quad (20)$$

where $b_1 > b_2 > c > 0$. When both players cooperate, the system either remains in or transitions to the prosperous state s_1 . Conversely, if at least one player defects, the system collapses to the degraded state s_2 .

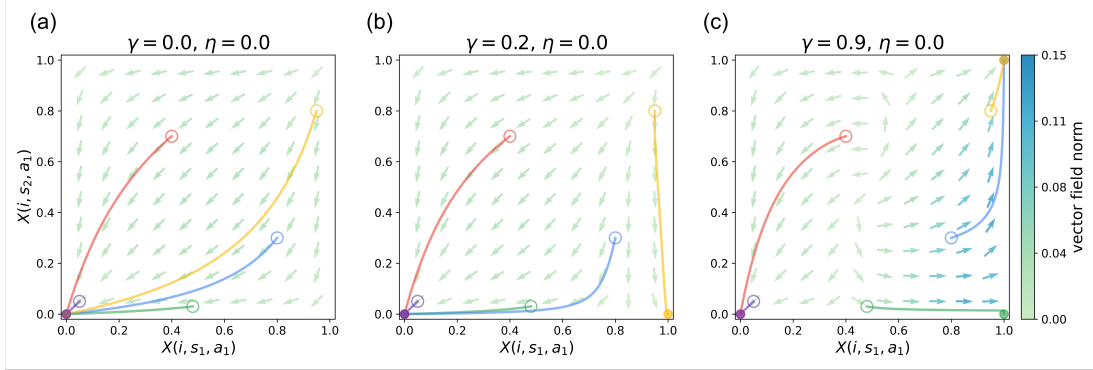


Figure 4: Vector fields and numerical simulation trajectories for the two-state Prisoner's Dilemma game without entropy regularization. The x-axis is the cooperation probability of both agents in state s_1 , and the y-axis is the cooperation probability in state s_2 .

For normal-form Prisoner's Dilemma games, namely, without state transition, the two players always converge to mutual defection [18, 3, 23]. Intuitively, cooperation imposes a personal cost c on the player and delivers a benefit b_k to the co-player, whereas defection leaves both players unaffected. Consequently, regardless of what the co-player does, the rational choice is always to defect. However, mutual cooperation yields a payoff of $b_k - c$ for each player, which exceeds the zero payoff from mutual defection. A key challenge is therefore to identify mechanisms that can steer the system towards mutual cooperation [5, 32]. The situation changes when state transitions are introduced: players must then balance short-term gains from defection against the risk of state degradation and the potential loss of long-term collective benefits. In the absence of entropy regularization, we summarize all possible stable equilibria of the system in Table 1 and present the corresponding dynamic regimes in Figure 4.

Stable equilibrium points ($\eta = 0$)	
Equilibrium point	Condition to be stable
\mathbf{X}_{0000}	always stable
\mathbf{X}_{1100}	$b_1/c > 1/\gamma$
\mathbf{X}_{1111}	$(b_1 - b_2)/c > 1/\gamma$

Table 1: Equilibrium points of the two-state Prisoner's Dilemma game without entropy regularization.

For convenience, we use subscripts to denote each agent's policy configuration. Specifically, \mathbf{X}_{uvxy} represents the agents' probabilities of selecting action a_1 in each state:

$$[X(1, s_1, a_1), X(2, s_1, a_1), X(1, s_2, a_1), X(2, s_2, a_1)] = [u, v, x, y]. \quad (21)$$

When the discount factor is low ($\gamma < c/b_1$), the system always converges to mutual defection, that is, \mathbf{X}_{0000} is globally stable. For myopic learning agents with small γ , future payoffs are largely ignored, and policy and value function updates depend primarily on immediate reward, as if agents learn in a normal-form game. As shown in Figure 4 (a), the vector field directs trajectories toward mutual defections, and all paths converge to this policy profile.

The equilibrium \mathbf{X}_{1100} become stable once the threshold $b_1/c = 1/\gamma$ is surpassed. In this equilibrium, agents cooperate in the prosperous state s_1 but defect in the degraded state s_2 . More

insights can be obtained through direct computation using Theorem 1. From the definition of \bar{Q} in Equation (8), the following identities hold for \mathbf{X}_{1100} :

$$\begin{aligned}\bar{Q}(i, s_1, a_1) &= b_1 - c + \gamma \bar{Q}(i, s_1, a_1) = (b_1 - c)/(1 - \gamma), \\ \bar{Q}(i, s_1, a_2) &= b_1 + \gamma \bar{Q}(i, s_2, a_2) = b_1, \\ \bar{Q}(i, s_2, a_1) &= -c, \\ \bar{Q}(i, s_2, a_2) &= 0.\end{aligned}\tag{22}$$

In the prosperous state s_1 , defection yields an immediate payoff of b_1 , whereas cooperation yields $(b_1 - c)/(1 - \gamma)$. In contrast, in the degraded state s_2 , defection always dominates cooperation, since the future reward term vanishes. Therefore, the equilibrium \mathbf{X}_{1100} is stable if and only if $\gamma > c/b_1$, which exactly reproduces the condition for direct reciprocity [32]. As shown in Figure 4 (b), the basin of attraction for \mathbf{X}_{1100} lies in the region where the cooperation probability $X(i, s_1, a_1)$ is high (see the yellow trajectory). In this regime, agents prefer to cooperate in the prosperous state s_1 to avoid the risk of mutual defection in the degraded state s_2 .

While the stability condition for \mathbf{X}_{1100} depends solely on the reward structure of state s_1 , it does not generalize to \mathbf{X}_{1111} . For this fully cooperative equilibrium, the incentive for agents to maintain cooperation in the degraded state s_2 stems from the potential to transition back to the prosperous state s_1 , where payoffs for cooperation are higher. Hence, a sufficiently large difference between the cooperative payoffs in the two states is necessary to motivate continued cooperation. The analytical stability condition $(b_1 - b_2)/c > 1/\gamma$ captures this intuition. As depicted in Figure 4 (c), the basins of attraction for \mathbf{X}_{1111} occupy the region where both agents maintain at least a decent level of cooperation in the prosperous state s_1 (see the yellow and blue trajectories).

5.2.1 Connection with Direct Reciprocity

The three equilibria listed in Table 1 parallel the classical strategies of direct reciprocity in EGT. Specifically, the equilibria \mathbf{X}_{0000} and \mathbf{X}_{1111} resemble the ALLD and ALLC strategies, respectively. Most intriguingly, the equilibrium \mathbf{X}_{1100} , where agents cooperate in the prosperous state s_1 but defect in the degraded state s_2 , is analogous to the GRIM strategy. As shown in Figure 5, GRIM agents cooperate until their opponent defects, after which they defect indefinitely. In the two-state PD, a co-player's defection triggers a transition to the degraded state s_2 , where the agents continued to defect under the \mathbf{X}_{1100} policy profile. The resulting behavior thus mirrors GRIM's pattern with striking fidelity.

The correspondence between strategies reveals a deeper structural relationship with the Iterated Prisoner's Dilemma (IPD). In the IPD, where agents repeatedly play a normal-form PD game, a memory-one player determines its next move based on the outcome of the previous round, represented by the four possible states {CC, CD, DC, DD}. The player's strategy $\mathbf{x} = [x_{CC}, x_{CD}, x_{DC}, x_{DD}]$ specifies the probability of choosing action a_1 in each state. Within the subspace defined by $x_{CD} = x_{DC} = x_{DD}$, the expected value \bar{Q} becomes identical across the states {CD, DC, DD}. Consequently, the evolutionary dynamics of x_{CD} , x_{DC} , and x_{DD} coincide. When the environment remains identical across the two environmental states, i.e., $b_1 = b_2$, the dynamics of the two-state PD game can therefore be viewed as a projection or homomorphic reduction of this subspace.

Furthermore, our framework highlights the critical role of environmental factors in sustaining cooperation. When $b_1 = b_2$, the incentive to escape the degraded state s_2 vanishes. While the stability of GRIM (\mathbf{X}_{1100}) remains unaffected, as it depends only on avoiding the immediate cost of defection in s_1 , the fully cooperative equilibrium ALLC (\mathbf{X}_{1111}) becomes unstable. In the absence of a higher reward for cooperation in s_1 , i.e., when $b_1 > b_2$, there is no long-term benefit to offset the immediate cost c of cooperating in the degraded state s_2 . Therefore, environmental heterogeneity emerges as a key mechanism for maintaining cooperation. The state-transition

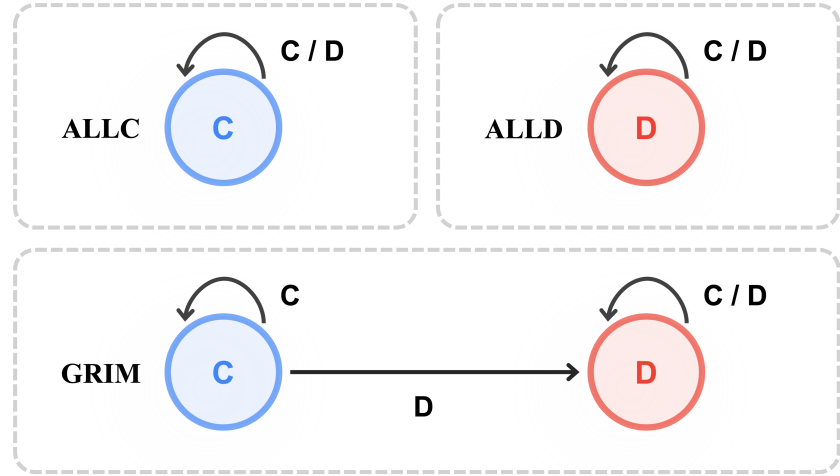


Figure 5: Finite-state automaton representations of three classical strategies in the iterated Prisoner’s Dilemma [6]. Each node represents an agent’s internal state (distinct from environmental states) and prescribes a specific action. The letters C and D denote cooperation (action a_1) and defection (action a_2), respectively. The arrows indicate transitions between internal states based on the opponent’s previous action. For the GRIM strategy, the initial internal state is C.

dynamics can enforce a form of reciprocity, where the “shadow of the future” is determined not only by the discount factor γ , but also by the threat of collective descent into a less prosperous environment and the shared incentive to regain mutual prosperity through cooperation.

5.2.2 Steering Control towards Stable Cooperation through Entropy Regularization

Although cooperation can be sustained under certain conditions, mutual defection always remains a stable equilibrium. Agents initialized with low probabilities of cooperation inevitably fall into mutual defection (see the red and purple trajectories in Figure 4). This dilemma can be mitigated by incorporating exploration via entropy regularization. The added stochasticity guides the system from a low level of cooperation toward an intermediate cooperative state, from which the exploitation process takes over and drives the dynamics to the cooperative equilibrium. As illustrated in Figure 6 (a), while a small fraction of cooperation at equilibrium is sacrificed, this trade-off ensures that the cooperative equilibrium point becomes globally stable. However, if the regularization strength is too large, the policy will degenerate into pure random behavior, as shown in Figure 6 (b).

6 Conclusion

In this work, we analyze the dynamics of entropy-regularized AC learning in stochastic games. By employing time-scale separation, we derive the ODEs that govern the evolution of agents’ policies, revealing a clear decomposition into exploitation and exploration components. Without entropy regularization, the system lacks an intrinsic mechanism for convergence and coordination, giving rise to diverse dynamical behaviors, including multistability and chaos.

As a matter of fact, entropy regularization plays a dual role in shaping agents’ behavior. On one hand, it promotes exploration, enabling agents to escape suboptimal local optima. In the two-state PD game, this mechanism expands the basin of attraction for the cooperative equilibrium, thereby alleviating the dilemma of mutual defection. From a dynamical systems perspective, entropy regularization enhances the system’s dissipativity. By incorporating an entropy term into the optimization process, the learning dynamics are driven toward smoother

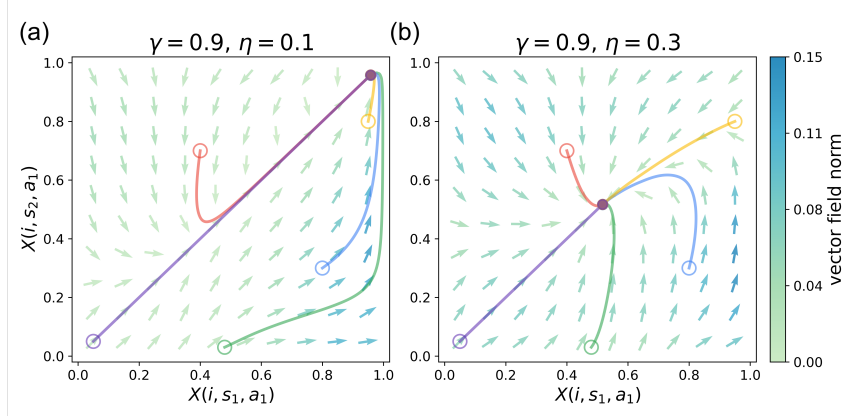


Figure 6: Vector fields and numerical simulation trajectories for the two-state Prisoner’s Dilemma game under entropy regularization.

and more robust regions of the policy space, which dampens unstable or chaotic dynamics and fosters stable and predictable trajectories.

Furthermore, our analysis uncovers a close connection between the emergence of cooperation in MARL systems and the mechanism of direct reciprocity in EGT. This connection motivates a multidisciplinary perspective that integrates insights from computer science, evolutionary biology, and physics [5]. By deepening our understanding of the fundamental rules that govern agents’ learning and adaptation, we can advance the design of robust, cooperative, and intelligent multi-agent systems [15].

References

- [1] Zafarali Ahmed, Nicolas Le Roux, Mohammad Norouzi, and Dale Schuurmans. Understanding the impact of entropy on policy optimization. In *International conference on machine learning*, pages 151–160. PMLR, 2019.
- [2] Robert Axelrod and William D Hamilton. The evolution of cooperation. *science*, 211(4489):1390–1396, 1981.
- [3] Wolfram Barfuss, Jonathan F Donges, and Jürgen Kurths. Deterministic limit of temporal difference reinforcement learning for stochastic games. *Physical Review E*, 99(4):043305, 2019.
- [4] Wolfram Barfuss, Jonathan F Donges, Vitor V Vasconcelos, Jürgen Kurths, and Simon A Levin. Caring for the future can turn tragedy into comedy for long-term collective action under risk of collapse. *Proceedings of the National Academy of Sciences*, 117(23):12915–12922, 2020.
- [5] Wolfram Barfuss, Jessica Flack, Chaitanya S Gokhale, Lewis Hammond, Christian Hilbe, Edward Hughes, Joel Z Leibo, Tom Lenaerts, Naomi Leonard, Simon Levin, et al. Collective cooperative intelligence. *Proceedings of the National Academy of Sciences*, 122(25):e2319948121, 2025.
- [6] Kenneth G Binmore and Larry Samuelson. Evolutionary stability in repeated games played by finite automata. *Journal of economic theory*, 57(2):278–305, 1992.
- [7] Tilman Börgers and Rajiv Sarin. Learning through reinforcement and replicator dynamics. *Journal of economic theory*, 77(1):1–14, 1997.

[8] Lucian Busoniu, Robert Babuska, and Bart De Schutter. A comprehensive survey of multi-agent reinforcement learning. *IEEE Transactions on Systems, Man, and Cybernetics, Part C (Applications and Reviews)*, 38(2):156–172, 2008.

[9] Ganqu Cui, Yuchen Zhang, Jiacheng Chen, Lifan Yuan, Zhi Wang, Yuxin Zuo, Haozhan Li, Yuchen Fan, Huayu Chen, Weize Chen, et al. The entropy mechanism of reinforcement learning for reasoning language models. *arXiv preprint arXiv:2505.22617*, 2025.

[10] Alhussein Fawzi, Matej Balog, Aja Huang, Thomas Hubert, Bernardino Romera-Paredes, Mohammadamin Barekatain, Alexander Novikov, Francisco J R. Ruiz, Julian Schrittwieser, Grzegorz Swirszcz, et al. Discovering faster matrix multiplication algorithms with reinforcement learning. *Nature*, 610(7930):47–53, 2022.

[11] Jakob Foerster, Ioannis Alexandros Assael, Nando De Freitas, and Shimon Whiteson. Learning to communicate with deep multi-agent reinforcement learning. *Advances in neural information processing systems*, 29, 2016.

[12] Jakob Foerster, Gregory Farquhar, Triantafyllos Afouras, Nantas Nardelli, and Shimon Whiteson. Counterfactual multi-agent policy gradients. In *Proceedings of the AAAI conference on artificial intelligence*, volume 32, 2018.

[13] James W Friedman. A non-cooperative equilibrium for supergames. *The Review of Economic Studies*, 38(1):1–12, 1971.

[14] Tuomas Haarnoja, Aurick Zhou, Pieter Abbeel, and Sergey Levine. Soft actor-critic: Off-policy maximum entropy deep reinforcement learning with a stochastic actor. In *International conference on machine learning*, pages 1861–1870. Pmlr, 2018.

[15] Lewis Hammond, Alan Chan, Jesse Clifton, Jason Hoelscher-Obermaier, Akbir Khan, Euan McLean, Chandler Smith, Wolfram Barfuss, Jakob Foerster, Tomáš Gavenčiak, et al. Multi-agent risks from advanced ai. *arXiv preprint arXiv:2502.14143*, 2025.

[16] Daniel Hennes, Michael Kaisers, and Karl Tuyls. Resq-learning in stochastic games. In *Adaptive and Learning Agents Workshop at AAMAS*, page 8. Citeseer, 2010.

[17] Daniel Hennes, Karl Tuyls, and Matthias Rauterberg. State-coupled replicator dynamics. In *AAMAS (2)*, pages 789–796, 2009.

[18] Christian Hilbe, Štěpán Šimsa, Krishnendu Chatterjee, and Martin A Nowak. Evolution of cooperation in stochastic games. *Nature*, 559(7713):246–249, 2018.

[19] Shuyue Hu, Chin-wing Leung, and Ho-fung Leung. Modelling the dynamics of multiagent q-learning in repeated symmetric games: a mean field theoretic approach. *Advances in Neural Information Processing Systems*, 32, 2019.

[20] Shuyue Hu, Chin-Wing Leung, Ho-fung Leung, and Harold Soh. The dynamics of q-learning in population games: A physics-inspired continuity equation model. In *Proceedings of the 21st International Conference on Autonomous Agents and Multiagent Systems*, pages 615–623, 2022.

[21] Lorens A Imhof and Martin A Nowak. Stochastic evolutionary dynamics of direct reciprocity. *Proceedings of the Royal Society B: Biological Sciences*, 277(1680):463–468, 2010.

[22] Natasha Jaques, Angeliki Lazaridou, Edward Hughes, Caglar Gulcehre, Pedro Ortega, DJ Strouse, Joel Z Leibo, and Nando De Freitas. Social influence as intrinsic motivation for multi-agent deep reinforcement learning. In *International conference on machine learning*, pages 3040–3049. PMLR, 2019.

- [23] Ardeshir Kianercy and Aram Galstyan. Dynamics of boltzmann q learning in two-player two-action games. *Physical Review E—Statistical, Nonlinear, and Soft Matter Physics*, 85(4):041145, 2012.
- [24] Vijay Konda and John Tsitsiklis. Actor-critic algorithms. *Advances in neural information processing systems*, 12, 1999.
- [25] Daeyeol Lee, Michelle L Conroy, Benjamin P McGreevy, and Dominic J Barraclough. Reinforcement learning and decision making in monkeys during a competitive game. *Cognitive brain research*, 22(1):45–58, 2004.
- [26] Joel Z. Leibo, Vinicius Zambaldi, Marc Lanctot, Janusz Marecki, and Thore Graepel. Multi-agent reinforcement learning in sequential social dilemmas. In *Proceedings of the 16th Conference on Autonomous Agents and MultiAgent Systems*, AAMAS ’17, page 464–473, Richland, SC, 2017. International Foundation for Autonomous Agents and Multiagent Systems.
- [27] Michael L Littman. Markov games as a framework for multi-agent reinforcement learning. In *Machine learning proceedings 1994*, pages 157–163. Elsevier, 1994.
- [28] Eric Mazumdar, Lillian J Ratliff, Michael I Jordan, and S Shankar Sastry. Policy-gradient algorithms have no guarantees of convergence in linear quadratic games. In *Proceedings of the 19th International Conference on Autonomous Agents and MultiAgent Systems*, pages 860–868, 2020.
- [29] Richard D McKelvey and Thomas R Palfrey. Quantal response equilibria for normal form games. *Games and economic behavior*, 10(1):6–38, 1995.
- [30] Volodymyr Mnih, Adria Puigdomenech Badia, Mehdi Mirza, Alex Graves, Timothy Lillicrap, Tim Harley, David Silver, and Koray Kavukcuoglu. Asynchronous methods for deep reinforcement learning. In *International conference on machine learning*, pages 1928–1937. PMLR, 2016.
- [31] Kamal K Ndousse, Douglas Eck, Sergey Levine, and Natasha Jaques. Emergent social learning via multi-agent reinforcement learning. In *International conference on machine learning*, pages 7991–8004. PMLR, 2021.
- [32] Martin A Nowak. Five rules for the evolution of cooperation. *science*, 314(5805):1560–1563, 2006.
- [33] Ann Nowé, Peter Vrancx, and Yann-Michaël De Hauwere. Game theory and multi-agent reinforcement learning. In *Reinforcement learning: State-of-the-art*, pages 441–470. Springer, 2012.
- [34] Long Ouyang, Jeffrey Wu, Xu Jiang, Diogo Almeida, Carroll Wainwright, Pamela Mishkin, Chong Zhang, Sandhini Agarwal, Katarina Slama, Alex Ray, et al. Training language models to follow instructions with human feedback. *Advances in neural information processing systems*, 35:27730–27744, 2022.
- [35] HL Prasad, Prashanth LA, and Shalabh Bhatnagar. Two-timescale algorithms for learning nash equilibria in general-sum stochastic games. In *Proceedings of the 2015 International Conference on Autonomous Agents and Multiagent Systems*, pages 1371–1379, 2015.
- [36] Stuart Russell and Peter Norvig. *Artificial Intelligence: A Modern Approach*. Prentice Hall, 3 edition, 2010.

[37] John Schulman, Sergey Levine, Pieter Abbeel, Michael Jordan, and Philipp Moritz. Trust region policy optimization. In *International conference on machine learning*, pages 1889–1897. PMLR, 2015.

[38] John Schulman, Filip Wolski, Prafulla Dhariwal, Alec Radford, and Oleg Klimov. Proximal policy optimization algorithms. *arXiv preprint arXiv:1707.06347*, 2017.

[39] Sofia Sgroi, G Massimo Palma, and Mauro Paternostro. Reinforcement learning approach to nonequilibrium quantum thermodynamics. *Physical Review Letters*, 126(2):020601, 2021.

[40] Lloyd S Shapley. Stochastic games. *Proceedings of the national academy of sciences*, 39(10):1095–1100, 1953.

[41] David Silver, Guy Lever, Nicolas Heess, Thomas Degrif, Daan Wierstra, and Martin Riedmiller. Deterministic policy gradient algorithms. In *International conference on machine learning*, pages 387–395. Pmlr, 2014.

[42] David Silver, Julian Schrittwieser, Karen Simonyan, Ioannis Antonoglou, Aja Huang, Arthur Guez, Thomas Hubert, Lucas Baker, Matthew Lai, Adrian Bolton, et al. Mastering the game of go without human knowledge. *nature*, 550(7676):354–359, 2017.

[43] Richard S Sutton. Learning to predict by the methods of temporal differences. *Machine learning*, 3(1):9–44, 1988.

[44] Richard S. Sutton and Andrew G. Barto. *Reinforcement Learning: An Introduction*. The MIT Press, second edition, 2018.

[45] Josef Tkadlec, Christian Hilbe, and Martin A Nowak. Mutation enhances cooperation in direct reciprocity. *Proceedings of the National Academy of Sciences*, 120(20):e2221080120, 2023.

[46] Karl Tuyls and Ann Nowé. Evolutionary game theory and multi-agent reinforcement learning. *The Knowledge Engineering Review*, 20(1):63–90, 2005.

[47] Karl Tuyls, Katja Verbeeck, and Tom Lenaerts. A selection-mutation model for q-learning in multi-agent systems. In *Proceedings of the second international joint conference on Autonomous agents and multiagent systems*, pages 693–700, 2003.

[48] Peter Vrancx, Karl Tuyls, Ronald L Westra, and Ann Nowé. Switching dynamics of multi-agent learning. *AAMAS (1)*, 2008:307–313, 2008.

[49] Long Wang, Feng Fu, and Xingru Chen. Mathematics of multi-agent learning systems at the interface of game theory and artificial intelligence. *Science China. Information Sciences*, 67(6):166201, 2024.

[50] Zhen Wang, Chunjiang Mu, Shuyue Hu, Chen Chu, and Xuelong Li. Modelling the dynamics of regret minimization in large agent populations: a master equation approach. In *Ijcai*, volume 22, pages 534–540, 2022.

[51] Christopher JCH Watkins and Peter Dayan. Q-learning. *Machine learning*, 8(3):279–292, 1992.

[52] Yaodong Yang and Jun Wang. An overview of multi-agent reinforcement learning from game theoretical perspective. *arXiv preprint arXiv:2011.00583*, 2020.

[53] Chao Yu, Akash Velu, Eugene Vinitsky, Jiaxuan Gao, Yu Wang, Alexandre Bayen, and Yi Wu. The surprising effectiveness of ppo in cooperative multi-agent games. *Advances in neural information processing systems*, 35:24611–24624, 2022.

[54] Kaiqing Zhang, Zhuoran Yang, and Tamer Bǟsar. Multi-agent reinforcement learning: A selective overview of theories and algorithms. *Handbook of reinforcement learning and control*, pages 321–384, 2021.